RESEARCH & INNOVATION DIVISION
IJIST

Evaluating and Predicting the Land Use Land Cover Changes and its Impact on Land Surface Temperature using CA-Markov model: A study of District Mardan, Pakistan

Muhammad Awais Khan, Atta Ur Rahman, Zahid Khan, Zain Sultan, Faheema Marwat, Tabassum Naz, Bushra Zahid
Department of Geography & Geomatics (GIS/RS), University of Peshawar, Pakistan.

Citation | Khan. M. A, Rahman. A. U, Khan. Z, Sultan. Z, Marwat. F, Naz. T, Zahid. B, "Evaluating and Predicting the Land Use Land Cover Changes and its Impact on Land Surface Temperature using CA-Markov model: A study of District Mardan, Pakistan", IJIST, Special Issue pp. 352-372, June 2024
Received | June 07, 2024; **Revised |** June 11, 2024; **Accepted |** June 14, 2024; **Published |** June 23, 2024.

Rapid population growth is a global phenomenon that alters landscapes and affects environmental conditions. The aim of this study is to find out the effects of urbanization on Land Use Land Cover (LULC) change and its impact on Land Surface Temperature (LST) in District Mardan from 2002 to 2022, and predicting LULC and surface temperature changes for future two decades (2042). The study uses remotely sensed data and Geographic Information Systems (GIS) to evaluate the correlation between the conversion of natural landscapes to built-up regions and the subsequent changes in LST. The key goals are to investigate LULC changes over the last two decades and examined the influence of LULC on LST and on the bases of these changes forecast the future LULC and LST trends using the CA-Markov model in IDRISI SILVA software for the year 2042. The examination of LULC changes from 2002 to 2022 found that built-up areas increased significantly and vegetation decreased. Built-up land increased from 10.10 % in 2002 to 16.28% in 2022, resulting in a 6% growth while vegetation covers experienced decreased by almost 10% of total Land cover. Similarly, in LST it is observed that more areas are getting prone to high temperature in 2022 relative to 2002. In 2002, 37% of total area experienced below 30° Celsius temperature while in 2022 it has dropped to 28% of total area. Additionally, by correlating LULC with LST it is evaluated that Barren surface and Built-up regions experienced high temperature. On the other hand, vegetation and water land parts of study area experienced low and moderate temperature. The CA-Markov model predicts that built-up land will increase by 19% in 2042, continuing the current trend and vegetation area of land will decrease by 4% of current status in 2022. Furthermore, the LST analysis indicates an increase in high temperature and low temperature regions are predicted to decrease further by another 3% of total study area as a result, the research shows that LST increases as built-up regions expand. This study not only illuminates the historical trajectory of urbanization and its thermal effects in District Mardan, but it also gives critical insights for sustainable land-use planning and urban heat island mitigation measures in the next decades.

Keywords: LULC; GIS; Land Surface Temperature; Urban Expansion; CA-Markov Chain Analysis.

Introduction:

The modification of Earth's terrestrial surface by human activities is commonly known as Land Use Land Cover (LULC) change around the globe [1]. The LULC is determined mainly by analyzing the ecological situation, geological structure, attitude, and slope, accompanied by the socio-economic, technological, and institutional set-up, which have greater influences on the land-use pattern in the area. The term Land Use Land Cover (LULC) refers to the ways in which land is used for agriculture, conservation, development, recreation, wildlife habitats, urban areas, or any other activity, as well as the results of human-environment interactions in a given area that are impacted by socioeconomic dynamics and climate change processes [2]. The change in the landscape can play an important role in changing the environment on a local as well as global scale [3]. Changes in land use and land cover are the outcome of both human activity and fast urban growth. The earth's surface has changed as a result of anthropological activities like population growth, fast urbanization, and economic advancement [4].

Since the settlement of the first human Mesopotamia between 4000 BC and 3000 BC, cities have been around for thousands of years. Now, more than half of the world's population can be found in urban areas. To achieve sustainability, humans are becoming city-dwelling' metro' sapiens'[5]. It is well known and documented that urbanization can have significant effects on local weather and climate. Urban climate studies have long been concerned about the magnitude of the difference in observed ambient air temperature between cities and their surrounding rural regions, which collectively describe the urban heat island (UHI) effect [5]. The main cause of UHI is from the modification of the land surface, and according to Ackerman, the urban temperature is 2–5 degrees higher than that in rural surroundings [6]. The intensity of land surface temperature is related to the patterns of land use and land cover changes like building roofs, paved surfaces, vegetation, bare ground, bare-ground and water [7]. Loss of vegetative cover by replacing it with built-up infrastructure causes Urban Heat Island (UHI), a term commonly used to describe the higher temperature in an urban area as compared to a rural setting. Such a situation has an adverse effect on the lives and daily activities of the urban population. Examined the LST pattern and its relationship with land cover in Guangzhou and in the urban clusters in the Zhejiang Delta, China. Studies using satellite-derived radiant temperature have been termed the surface temperature heat island [8].

The CA-Markov is a spatial transmutation model that combines the stochastic temporal Markov approach with the stochastic spatial cell division automata strategy for the simulation of temporal and spatial patterns of land use changes [9]. In the CA-Markov modeling process, the temporal changes of land use classes are directed in the Markov chain process based on the produced transition matrices [10]. Whereas, the spatial changes are controlled by transition potential maps, the configuration of neighborhoods, and local transition rules during the CA model process [11]. The CA-Markov chain model takes advantage of the Markov chain of land use change quantity prediction and dynamic explicit spatial simulation of the CA model [12]. The CA-Markov chain model takes advantage of the Markov chain of land use change quantity prediction and the dynamic explicit spatial simulation of the CA model [13]. Moreover, the CA–Markov model overcomes the lack of socioeconomic, statistical, and historical data [14].

Objectives:

- To find the land use land cover of study area and its change from 2002 to 2022 of the study area.
- To examine the spatial distribution and variations in LST across the study area and the impact of LULC on LST.
- To predict future LULC changes and LST for 2042 using CA-Markov model.

Novelty Statement:

The tittle of the current study is a novel idea of where LULC changes is a cause of human activity, so due to population increasing of the study area from 1981 to 2023 as par census report. The LULC changes should also be occurred, those LULC changes are impacting the Land Surface Temperature (LST) of the study area. The main purpose of this research is to find out the dynamics of LULC and the factors effecting LST. To find the recent dynamics and to predict the future on the basis of recent data changes using CA Markov model.

Material and Methods:

Study Area:

The study area Mardan district is part of Peshawar Valley, which first appears in history as part of the Gandhara Kingdom. Until 1937, Mardan district was a part of Peshawar district. In 1937, Mardan was set up as an independent district. The study area is situated between the latitudes of 34° 04' 40" to 34° 31' 51" north and the longitudes of 71° 49' 05" to 72° 26' 04" east. It is bounded on the north by Buner and Malakand districts, on the east by Swabi and Buner districts, on the south by Nowshera district, and on the west by Charsadda and Malakand districts as shown in Figure 1. The district overall geographic area is 1632 km^2 with a population of 1,460,100 on the basis of 1998 census report, which is increased to 2,373,399 in 2017 census report and further on the basis of 2023 census report the population was increased up to 2,744,898. However, the climatic conditions of the study area have been interpreted in light of the data recorded at Risalpur station, which is nearest to Mardan district and has more or less similar topographic conditions. The average temperature is 22.2 °C, while the annual precipitation averages 559 mm. Generally stream flows from north to the south. Most of the streams drain into Kabul River. Kalpani, an important stream of the district rises in the Baizai and flowing southwards join Kabul River. Other important streams which join Kalpani are Baghiari Khawar on the west and Muqam Khawar, coming from Sudham valley and Naranji Khawar from the Narangi hills on the left. The main source of irrigation water is the canals. The upper Swat canal irrigates most of the district, and the lower Swat canal irrigates south-western parts of the district. The other sources are tube wells and lift irrigation (GOP, 1998).

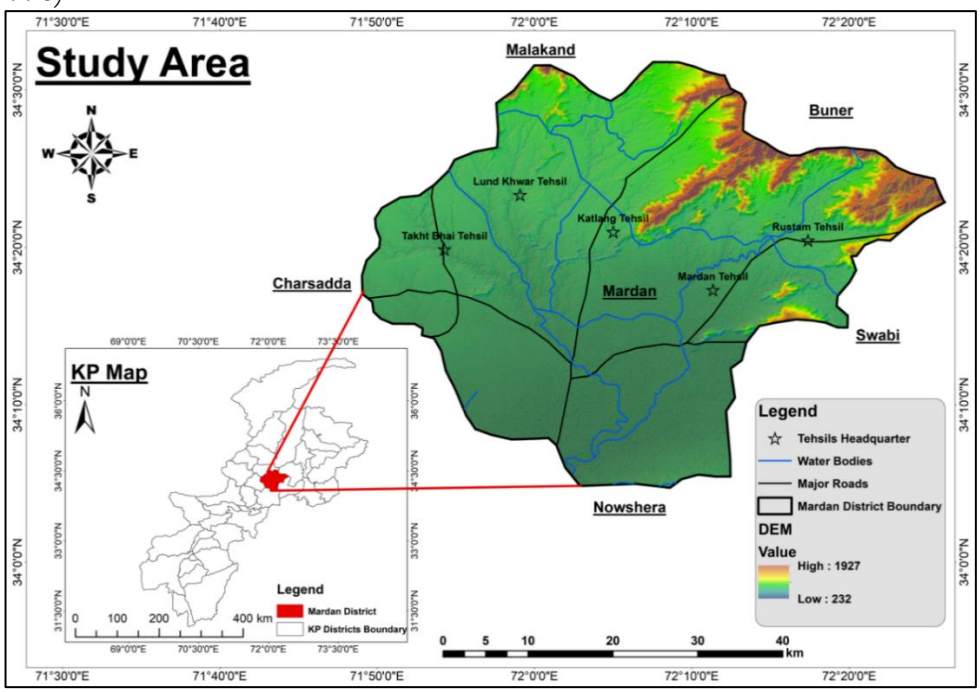

Figure 1: Location Map of the Study Area

Data Collection and Analysis:

The first step is data acquisition, the satellite Imageries are taken from USGS which is Landsat 7 and 8 for LULC and LST. The Second step (analysis) CA-Markov Chain was used for simulations of 2042 scenario. The CA-Markov is a cellular automata model in IDRISI Silva software which work on the basis of cells, so for simulations of 2042 scenario we use the past year data trend and changes. For past year data we use Markov who find the changes in data and on the bases of that data changes CA-Markov give simulation of future. The third step is to analyze the result of CA Markov, by analyzing the LULC and its direct impact on LST. The Fourth step was to correlate the LST with spectral/ satellite indices i.e. NDVI, NDBI, NDWI, SAVI, BI. In the Fifth step, the changes from prior year study were extracted and analyzed till the next study year.

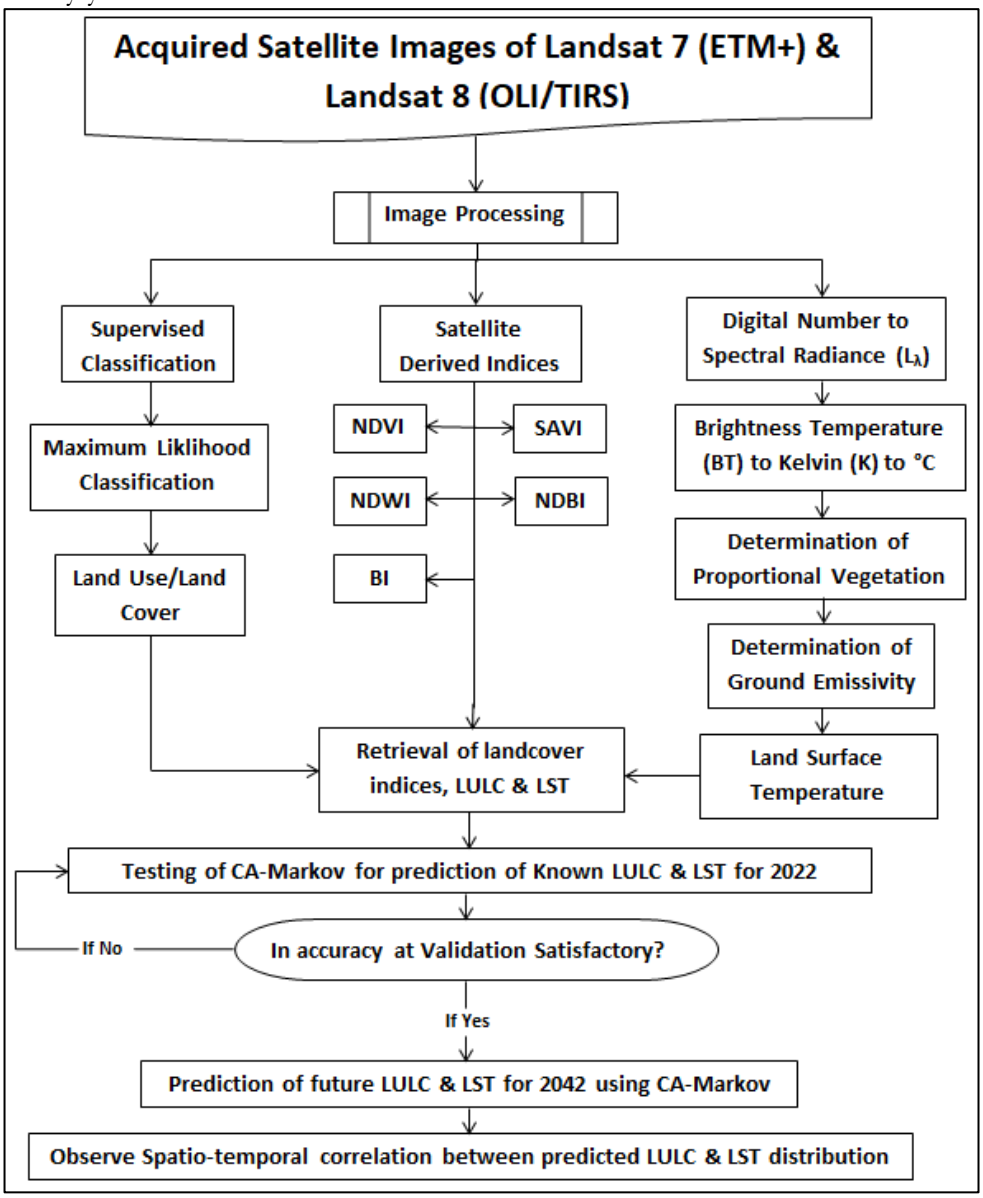

Figure 2: Flow Chart

Image Classification:

A maximum likelihood algorithm is the most common and popular method used for classification in remote sensing. Maximum probability classification requires a signature file with the (gsg) extension as an input. Maximum Likelihood Classification was used for the modification and correlation of each class signature. The goal of using MLC is to classify the

raster into different classes. Using this, a classified image is acquired, and the result is automatically classed as a raster in the arc map.

Extraction of LST from Thermal Band:

LST requires the conversion of sensor measurement to a physical quantity as a sensor records the intensity of electromagnetic radiation for each pixel as a digital number and we need to convert the Digital Numbers (DNs) to more meaningful real-world units like radiance (Watts), reflectance or brightness temperature. For extracting land surface temperature from thermal bands of Landsat imagery following procedure was followed.

Conversion of Digital Number (DN) to Spectral Radiance:

Every object with a temperature above absolute zero (k) emits thermal electromagnetic energy. Data received by thermal sensors can be converted to at-sensor radiance by using the radiance rescaling factors provided in the metadata file:

$$L_\lambda = M_L Q_{cal} + A_L \quad (1)$$

Where L_λ = TOA spectral radiance (Watts/ (m^2 * srad * μm); ML = Band-specific multiplicative rescaling factor from the metadata (RADIANCE_MULT_BAND_x, where x is the band number);

A_L =Band-specific additive rescaling factor from the metadata (RADIANCE_ADD_BAND_x, where x is the band number);

Q = Quantized and calibrated standard product pixel values (DN)

Conversion to At-Satellite Brightness Temperature:

Band data can then be converted from spectral radiance to top of atmosphere brightness temperature using the thermal constants provided in the metadata file by equation 2.

$$Tb = K*2 / \ln (k\,1 / L\lambda + 1) \quad (2)$$

Where T or BT = Top of atmosphere brightness temperature (K); L_λ = TOA spectral radiance (Watts/ (m2 * srad * μm); K_1 = Band-specific thermal conversion constant from the metadata (K1_CONSTANT_BAND_x, where x is the thermal band number); K_2 = Band-specific thermal conversion constant from the metadata (K2_CONSTANT_BAND_x, where x is the thermal band number).

Land Surface Temperature:

Land surface temperature was retrieved using a single channel algorithm, which makes use of a single thermal band of a dataset. Since the temperature obtained using the above-mentioned procedure is referenced to a blackbody, therefore corrections for land surface emissivity are necessary. Emissivity can be derived from normalized differentiated vegetative index. The emissivity corrected land surface temperature was derived using procedure proposed in equation 3.

$$LST = Tb / [1 + \{(\lambda * Tb / \varrho) * \ln\epsilon\}] \quad (3)$$

Where Tb = At - Satellite temperature; w = wavelength of emitted radiance; p= h * c / s (1.438 * 10^{-2} m K); h =Planck's constant (6.626 * 10^{-34} Js); s = Boltzmann Constant; c = velocity of light (2.998 * 10^8 m/s); e = Emissivity.

LSE or land surface emissivity can be defined as the ratio of the energy radiated from a material's surface to that radiated from a blackbody (a perfect emitter) at the same temperature and wavelength and under the same viewing conditions. It will be calculated by using the following equation:

$$LSE = 0.004 * PV + 0.986 \quad (4)$$

Where PV means proportion of vegetation and can be calculated using equation 5:

$$PV = \sqrt{(NDVI - NDVI_{min} / NDVI_{max} - NDVI_{min})}$$

Conversion of LST from Kelvin to Celsius the retrieved LST is in kelvin and its unit can be converted to Celsius using the relation 0 degree Celsius equals 273.15K. It can be done by using equation 5.

LST - 273.15 (5)

Result and Discussion:

Spatio-Temporal LULC Trend:

Findings shown in Figures 3 and 4 how land use and land cover (LULC) changed in the Mardan district between 2002 and 2022. Significant changes in the built-up area in the city's center region in 2002 are seen in Figure 3, which suggests an early stage of urban growth. As Figure 4 illustrates, there was a discernible rise in the built-up area by 2022, with the majority of this growth occurring in the district center. There was also a low vegetation index at this time, which was probably caused by less rainfall. Smaller built-up areas also started to emerge all throughout the region, suggesting irregular urban expansion. The built-up area is significantly amplified, which may be attributed to the implementation of many housing plans in Mardan and its neighboring cities between 2002 and 2022. Mardan and its surrounding cities saw a significant decline in their plant cover as a result of this fast urbanization, highlighting the trade-off between growing cities and green areas. A quantitative summary of the major changes in the LULC distribution between 2002 and 2022 using the Maximum Likelihood Classification (MLC) algorithm is presented in Table 1. The data shows that between 2002 and 2022, there was a significant increase in the built-up area, with the most prominent changes occurring in agricultural and vegetative fields and urban settings.

In particular, from 165.47 km^2 (10.10% of the total area) to 266.70 km^2 (16.28%), the built-up area increased significantly. At the same time, there were decreases in areas of vegetation and a slight increase or stability somehow in bare terrain. While increasing water bodies from 25.03 km^2 (1.53%) to 49.61 km^2 (3.03%), a slight increase in barren land from 518.60 km^2 (31.67%) to 528.46 km^2 (32.27%), and lowering vegetative areas from 928.76 km^2 (56.70%) to 793.09 km^2 (48.42%).

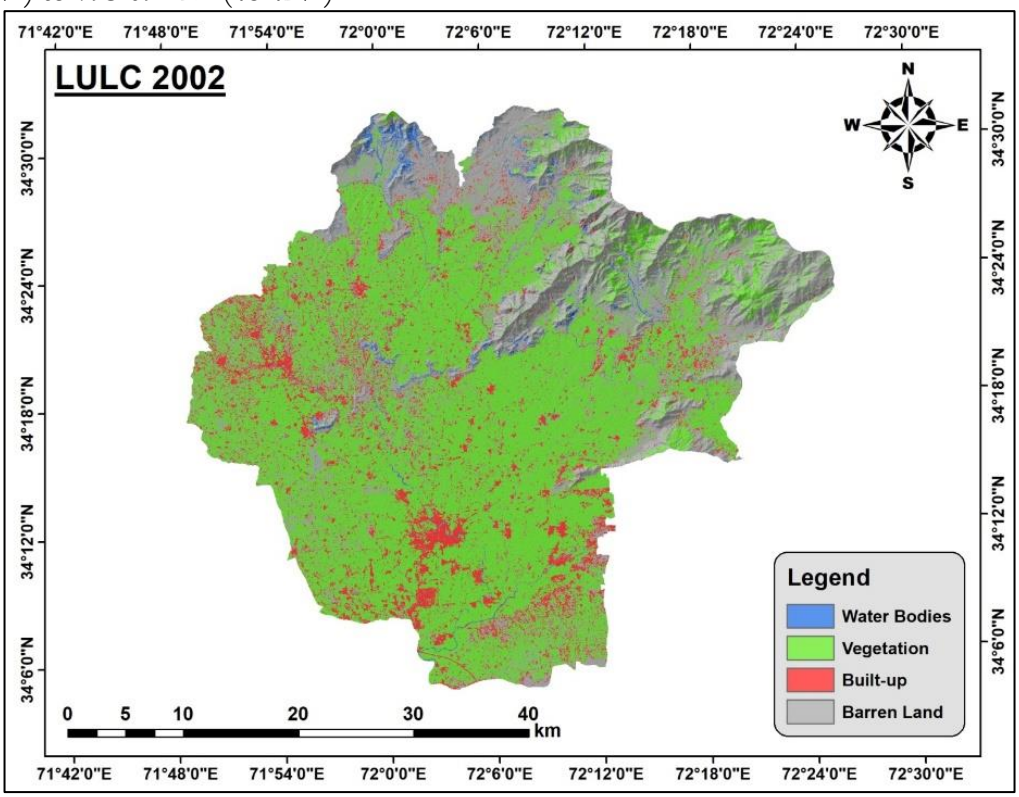

Figure 3: LULC of District Mardan 2002

Spatio-Temporal Changes in LULC from 2002 to 2022:

Over the course of 20 years, from 2002 to 2022, the Mardan district's land use and land cover (LULC) changed significantly across a number of land cover categories. Excluding

unaltered regions, this research uses statistical data and geographical maps to show how the landscape evolved.

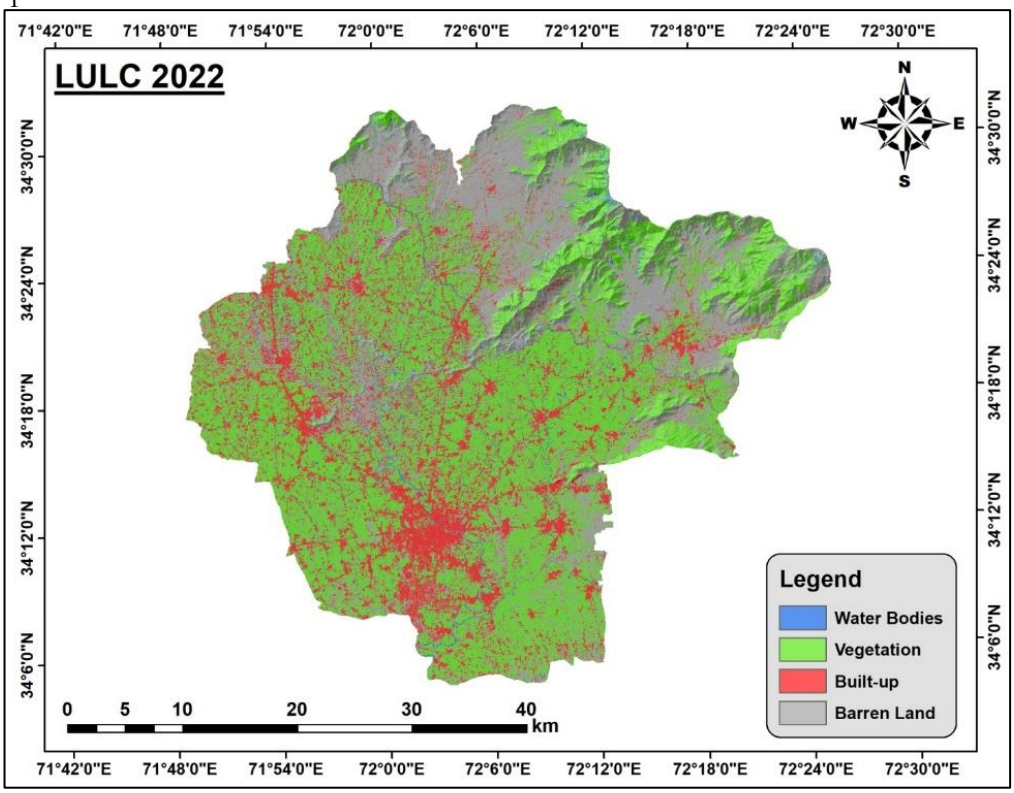

Figure 4: LULC of District Mardan 2022

Table 1: Temporal changes of LULC from 2002 to 2022

LULC	2002		2022	
Classes Names	**Area in Km²**	**%**	**Area in Km²**	**%**
Water Bodies	25.03	1.53	49.61	3.03
Vegetation	928.76	56.71	793.09	48.42
Built-up	165.47	10.10	266.70	16.28
Barren Land	518.60	31.66	528.46	32.27

Barren Land (BA) to Built-up Land (BU):

About 50.70 km^2, or around 3.10% of the total area, of undeveloped land was turned into built-up land between 2002 and 2022. This changeover is indicative of the growth of cities and the improvement of their infrastructure throughout the last 20 years. The building of residential, commercial, and industrial structures, spurred by economic expansion and population growth, is the main cause of the increase in built-up areas. These changes may be seen on the map in the orange patches, which show where urbanization has taken over territory that was either not used or had very little vegetation.

Barren Land (BA) to Vegetation Land (VG):

About 177.63 km^2, or 10.85% of the overall area, is now vegetated, which is a significant change from the formerly desolate terrain. Efforts to reforest, expand agriculture, or restore natural vegetation might all contribute to this change. In order to improve ecological balance, boost biodiversity, and reduce soil erosion, it is essential to increase plant cover. More and more people are realizing the value of parks and other green areas, and this shift reflects that.

Barren Land (BA) to Water Bodies (WB):

A less dramatic but nevertheless noticeable alteration is the incorporation of bodies of water into an area of around 12.38 km^2 (0.76% of the overall area). This can be because of new

water management projects like ponds or reservoirs that were built to accommodate irrigation demands and increase water availability. Even while these improvements aren't as big as others, they're nonetheless important for the district's water resource management.

Vegetation Land (VG) to Barren Land (BA):

On the flip side, 95.59 km^2, or 5.84% of the whole area, have gone from being vegetated to being desert. Reasons for this deterioration include the loss of vegetation due to natural catastrophes, overgrazing, unsustainable farming methods, or deforestation. Together, we can rehabilitate degraded regions and apply sustainable land management approaches to solve these problems.

Vegetation Land (VG) to Built-up Land (BU):

Red patches on the map represent areas that have been developed from vegetation, which accounts for around 146.16 km^2 (8.93% of the overall area). The continuous development of housing and commercial spaces in once agricultural or wooded regions is a reflection of this tendency in urban sprawl. Even if this is a sign of economic prosperity, it also highlights the need of well-planned metropolitan areas that manage expansion while preserving the environment.

Water Bodies (WB) to Barren Land (BA):

The transformation of around 1.97 km^2 of aquatic bodies into undeveloped land, accounting for 0.12% of the total area, is a small but notable alteration. The depletion of water supplies, sedimentation, or the drying up of bodies of water as a consequence of climate change are all potential causes of this alteration. The hydrological equilibrium and local ecosystems depend on the preservation of existing water bodies.

Water Bodies (WB) to Vegetation Land (VG):

Lastly, spots where water bodies have either diminished in size or been filled in, resulting in the growth of vegetation, may be shown by converting around 0.96 square kilometers, or 0.06% of the overall area, of water bodies into terrestrial vegetation. While this may have positive effects on native species, it also draws attention to the necessity to track shifts in the availability of water resources.

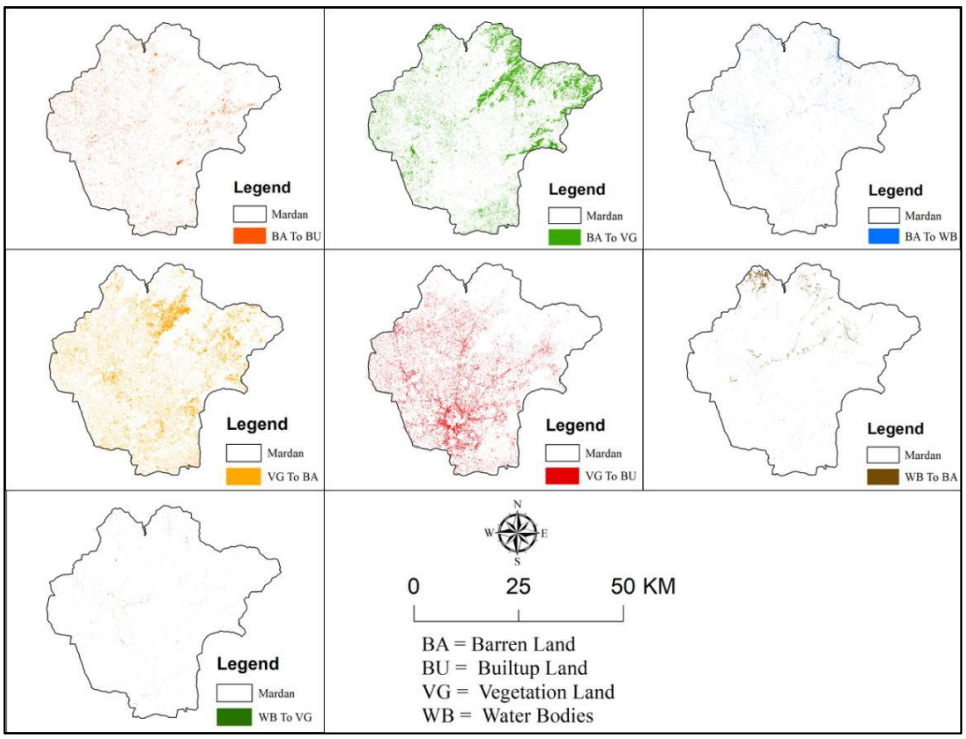

Figure 5: Maps of LULC change from 2002 to 2022

Table 2: Change in LULC statistics from 2002 to 2022

Class 2002	Class 2022	Change Classes	Change Area Sq.km	Change %
Barren Land	Barren Land	No change	273.17	16.69
Barren Land	Built-up	BA To BU	50.70	3.10
Barren Land	Vegetation	BA To VG	177.63	10.85
Barren Land	Water Bodies	BA To WB	12.38	0.76
Built-up	Built-up	No change	161.23	9.85
Vegetation	Barren Land	VG To BA	189.09	11.55
Vegetation	Built-up	VG To BU	128.82	7.87
Vegetation	Vegetation	No change	620.76	37.92
Water Bodies	Barren Land	WB To BA	15.76	0.96
Water Bodies	Vegetation	WB To VG	2.72	0.17
Water Bodies	Water Bodies	No change	4.60	0.28

Observed LST from 2002 to 2022 Using Landsat Data:

Since 2002, the long-term Land Surface Temperature (LST) in Mardan district has increased noticeably. This pattern is seen in Figure 6 and 7, which also shows that in 2002, the region's average temperature fell between 28 and 31 °C and 31 and 33 °C. The most prevalent temperature range, however, has changed by 2022, with the 31–33 °C and 33–35 °C as well as 35 - 41 °C group becoming the most common. The Land Surface Temperature (LST) in Mardan district was recorded in 2002, and it ranged from 25°C to 36°C, suggesting a considerable variance in temperature throughout the area. By 2022, though, this temperature range had greatly increased, reaching 20°C to 41 °C. This sharp rise draws attention to the wider range of temperatures and emphasizes how hot it is getting, especially in cities.

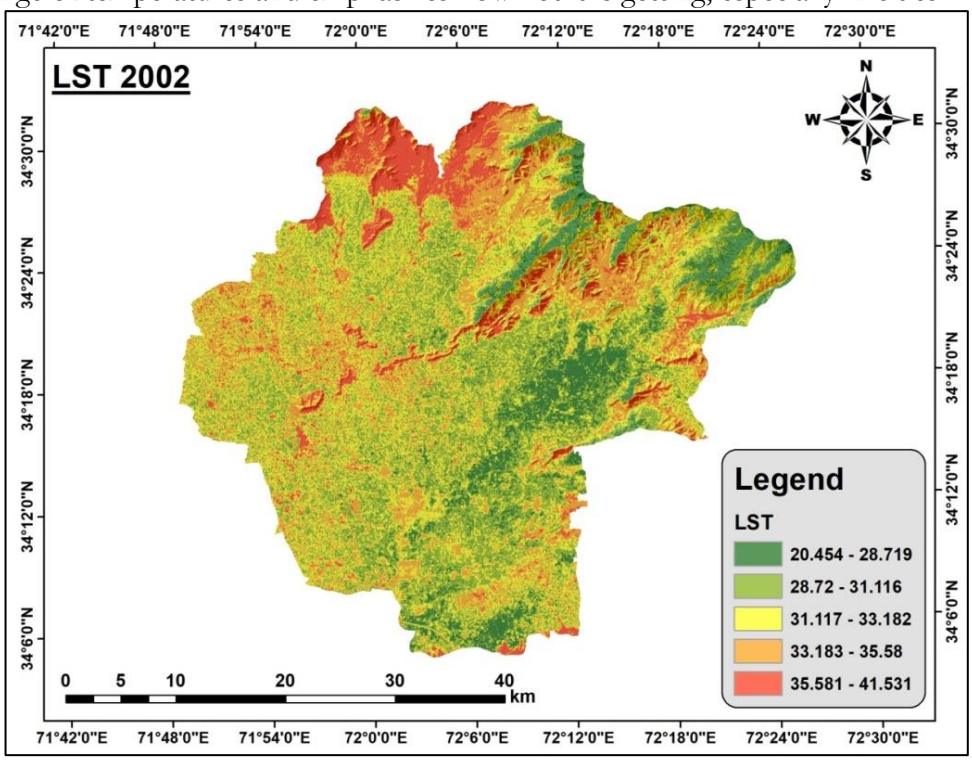

Figure 6: LST Map of 2002

The data for 2022 in Figure 8 demonstrate a temperature increase that extends towards the borders, raising the temperature over a sizable area of the city. Between 31 and 35 °C and 35 and 41 °C were the temperatures experienced by around one-third of the city. The regions with greater temperatures increased throughout time, whereas the area with lower temperatures shrank. While most of the region had temperatures between 20 and 28 °C in

2002, Mardan City saw temperatures reach 35 – 41 °C by 2022. This shows that over a 20-year period, temperatures have risen by up to 12 °C. An overview of the changes in LST between 2002 and 2022 may be seen in Table 3. As the city grew the proportion of places with temperatures between 20 and 23 °C decreased by around 3% throughout this time. Furthermore, there was a notable rise of 4% in the coverage of high LSTs (35–41 °C), indicating that Mardan City has likely been subjected to significant surface warming during the previous few decades.

Table 3: Temporal trend of LST observed in 2002 & 2022

LST	2002		2022	
Classes Names	**Area in km²**	**%**	**Area in km²**	**%**
20.454 - 28.719	147.94	9.03	100.05	6.11
28.72 - 31.116	466.99	28.51	360.95	22.05
31.117 - 33.182	511.98	31.26	493.15	30.13
33.183 - 35.58	362.40	22.13	426.59	26.06
35.581 - 41.531	148.54	9.07	256.14	15.65

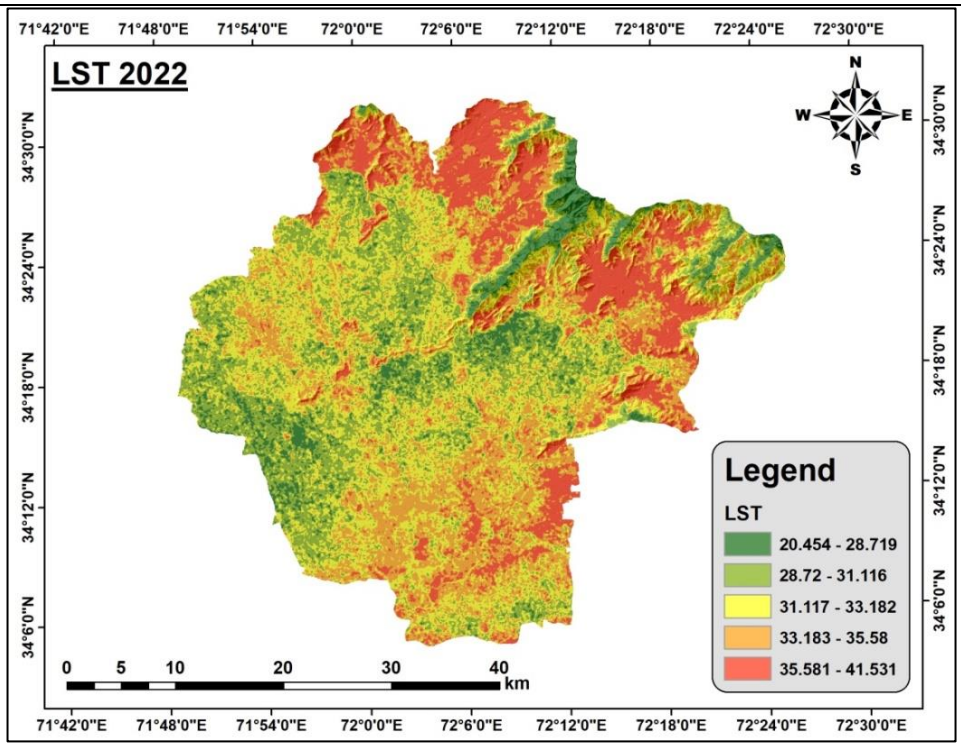

Figure 7: LST Map of 2022

Spatio-Temporal Changes in LST from 2002 to 2022:

Significant transitions between various temperature classes are shown by the examination of the change in Land Surface Temperature (LST) in District Mardan of Khyber Pakhtunkhwa from 2002 to 2022. For efficient environmental management and policy making, it is essential to comprehend the geographical and temporal dynamics of LST changes.

District Mardan Land Surface Temperature (LST) data shows a general upward trend from 2002–2022. Moving from lower to higher temperature classes is more noticeable, with large regions shifting from "Very Low" (VL) and "Low" (L) to "Medium" (M), "High" (H), and "Very High" (VH). Around 519.70 km² of the region has gone from a colder to a warmer temperature class overall. On the other side, a region covering around 218.49 km² has cooled, shifting from a warmer to a colder class. As a result of urbanization, changes in land use, and other human-caused variables, the district as a whole had a net rise in temperatures throughout the 20-year period. Detailed overviews of the transitions of LST classes are given below.

Very Low LST class to Other LST Classes:

The "Very Low" (VL) temperature class showed the most consistent change, with 37.10 km² of the region remaining in this category (2.27% of the total area). Areas with this level of stability have not seen major shifts in temperature within the last 20 years. On the other side, there were clear shifts from "Very Low" to other categories, indicating hotter spots. In particular, 2.50% of the total land, or 40.94 km², went from VL to "Low" (L), while 2.28% of the area, or 37.39 km², went from VL to "Medium" (M). These shifts point to a district-wide trend toward more moderate warming. Upon further examination, it was determined that 25.44 km², constituting 1.55% of the region, went from VL to "High" (H) temperature. A much lower but still substantial 6.04 km², or 0.37 percent of the whole area, was moved from VL to "Very High" (VH). The most rapidly warming areas are being highlighted by these increases, which may be attributable to human activities like urbanization, deforestation, or shifts in land use.

Low LST Class to Other LST Classes:

A variety of transitions are displayed by the "Low" (L) temperature set: A total area of 28.32 km² went from Low to Very Low LST class, making up 1.73% of the entire area shows positive change. This suggests that certain areas are cooling off, which might be because of reforestation or less human activity. A considerable percentage, 129.69 km² (7.92%), stayed within the Low class, indicating regions with minimal temperature change. The switch from Low (L) to Medium (M) occurred in 172.25 km², or 10.52 percent of the total, demonstrating that these areas experienced moderate warming, most likely as a result of urbanization or agricultural practices. The fact that 107.25 km² (6.55%) shifted from low (L) to high (H) suggests considerable warming, which may be the result of increased new infrastructure. A total of 30.44 km², or 1.86%, moved from low to very high, drawing attention to regions where temperatures have risen sharply as a result of widespread changes in land use.

Moderate LST Class to Other LST Classes:

A wide variety of transitions, representing both rising and falling temperatures, make up the "Moderate" (M) temperature class. It is possible that efficient land management techniques are to reason for the substantial cooling of around 21.06 km² (1.29%) between M and VL. A little cooling tendency, probably associated with better land cover or weather, is suggested by another noteworthy transition, this one from M to L, which covers 133.53 km² (8.16%). Almost all of the area, 180.15 km² or 11.01%, stayed in the M class, indicating that there was minimal temperature fluctuation and that these areas likely have balanced elements influencing temperature. On the other hand, a substantial chunk of 131.41 km² (8.03%) went from M to "High" (H), indicating major warming tendencies most likely caused by growing industrialization and urbanization. Furthermore, 48.22 km², or 2.95% of the area, crossed over to "Very High" (VH), suggesting regions of extremely high temperatures, perhaps caused by heightened human activity and environmental deterioration. These changes from the M class show that the district's temperature changes have been very uneven, with some places seeing markedly higher temperatures and others seeing markedly lower one.

High LST Class to Other LST Classes:

The temperature class transitions labeled as "High" (H) indicate notable environmental effects. Approximately 9.75 square kilometers, which accounts for 0.60% of the whole area, saw a decrease in temperature from high to very low levels. This suggests that certain regions were successful in effectively lowering temperatures. In addition, an area of 50.90 square kilometers (3.11% of the total) had a shift from high to low temperatures, indicating slight cooling tendencies. A few regions, encompassing 92.68 km² (5.66% of the total area), transitioned from a hotter climate zone (H) to a moderately hot climate zone (M). This shift was accompanied by a minor decrease in temperature, which might perhaps be attributed to the implementation of more effective land management techniques or the implementation of

initiatives aimed at conserving the environment. Despite the decreases, a total area of 118.63 square kilometers (7.25% of the total) remained steady within the H class, suggesting minimal temperature change. An evident shift from H to "Very High" (VH) is apparent, with 88.94 km² (5.43%) representing regions seeing a significant increase in temperature, most likely as a result of greater urbanization and changes in land use.

Very High LST Class to Other LST Classes:

To understand the areas most impacted, it is necessary to look at the "Very High" (VH) temperature class changes. As a result of the effective environmental restoration activities, around 3.03 km² (0.19%) cooled dramatically from VH to VL. There was a change from VH to L of 6.13 km² (0.37%), which might indicate cooling trends in some areas. The mild cooling impacts were shown by a few regions that changed from VH to M, covering 11.89 km² (0.73%). There is a significant change from VH to H, though, with 43.85 km² (2.68%) indicating regions that cooled marginally but are still in the upper temperature categories. Finally, there was minimal temperature change in a large area, 81.82 km² (5.00%), which stayed in the VH class.

Table 4: LST Changes in Classes from 2002 - 2022

Class 2002	Class 2022	Change Classes	Change Area SqKm	Change %
VL	VL	VL To VL	37.10	2.27
VL	L	VL To L	40.94	2.50
VL	M	VL To M	37.39	2.28
VL	H	VL To H	25.44	1.55
VL	VH	VL To VH	6.04	0.37
L	VL	L To VL	28.32	1.73
L	L	L To L	129.69	7.92
L	M	L To M	172.25	10.52
L	H	L To H	107.25	6.55
L	VH	L To VH	30.44	1.86
M	VL	M To VL	21.06	1.29
M	L	M To L	133.53	8.16
M	M	M To M	180.15	11.01
M	H	M To H	131.41	8.03
M	VH	M To VH	48.22	2.95
H	VL	H To VL	9.75	0.60
H	L	H To L	50.90	3.11
H	M	H To M	92.68	5.66
H	H	H To H	118.63	7.25
H	VH	H To VH	88.94	5.43
VH	VL	VH To VL	3.03	0.19
VH	L	VH To L	6.13	0.37
VH	M	VH To M	11.89	0.73
VH	H	VH To H	43.85	2.68
VH	VH	VH To VH	81.82	5.00

Measurement of Coefficient of Determination for LST with Normalized Satellite Indices: Table 3.7 shows the Mardan region's annual fluctuation in LST for the years 2002 and 2022 according to several normalized satellite indexes. According to the statistics, the yearly variability of LST has significantly increased throughout the last two decades. When compared to indices like the Normalized Difference Built-up Index (NDBI), Soil Adjusted Vegetation Index (SAVI), Normalized Difference Vegetation Index (NDVI), and Bare Soil Index (BI), this fluctuation is much more obvious on a yearly basis.

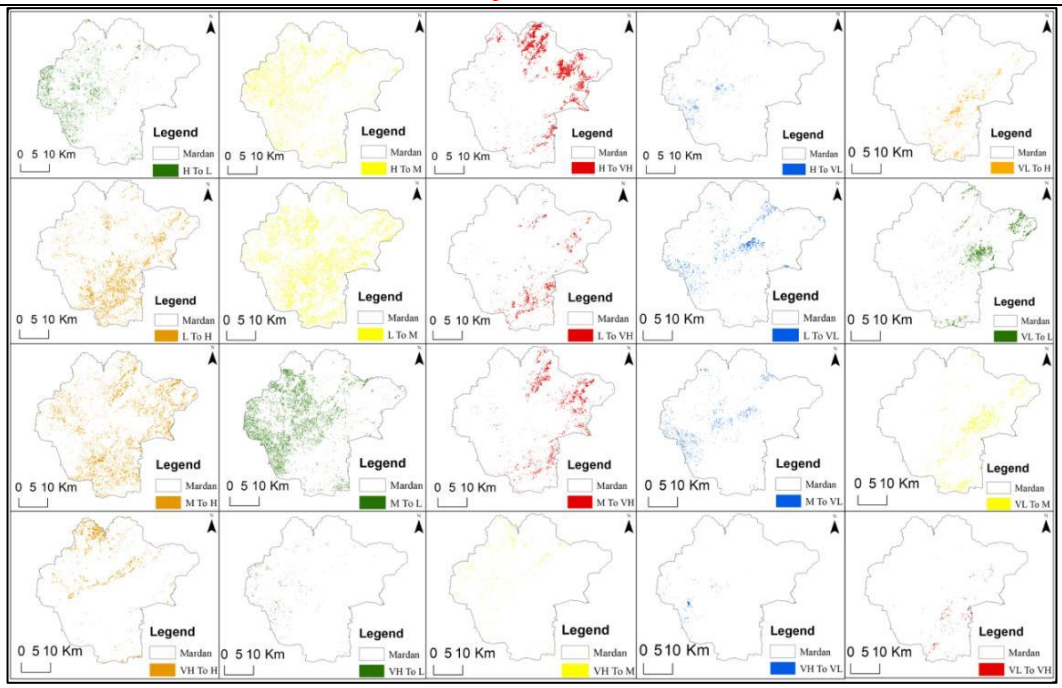

Figure 8: LST Changes in Classes from 2002 – 2022

LST and indicators like SAVI, NDBI, and BI showed a statistically significant positive association from 2002 to 2022, especially in Mardan City. This implies that the LST grew along with urbanization and soil exposure, implying greater temperatures in these less vegetated and built-up regions. On the other hand, there was a negative correlation found between LST and NDVI and NDWI, suggesting that cooler temperatures were often found in places with more vegetation and water. This pattern emphasizes how greenery and sources of water reduce urban heat.

There have been unfavorable trends in LST in Mardan western and higher regions. The importance of green cover in reducing urban heat is shown by the fact that the absence of vegetation in certain areas has greatly increased temperatures. On the other hand, a tiny area in Mardan's eastern and lower region showed an inverse association with NDVI. Because of this scant vegetation, it was more difficult to precisely assess LST patterns in this area.

All things considered, the robust relationship seen between LST and the many indices evaluated on an annual basis highlights the intricate relationship among surface temperatures, vegetation cover, and urban growth. By 2022, the association between LST and these indicators showed a 75.4% rise in positive trends. This shows that variations in these indicators have a considerable effect on the LST, indicating the importance of environmental variables and urbanization on Mardan's temperature fluctuation.

LST and NDVI:

2002: There is a substantial negative connection (R^2 = -0.6530) between LST and NDVI. Lower LST levels are correlated with higher NDVI values, which indicate more thick vegetation. This implies that vegetation aids in surface cooling. **2022**: There is still a negative association, but it is less evident as the correlation drops to −0.5453. This suggests that the cooling impact of vegetation is diminishing, maybe as a result of urban growth limiting the amount of green space.

LST and NDWI:

2002: There is a somewhat favorable connection (R^2 = 0.4140) between LST and NDWI. This seems a little odd because bodies of water usually have a cooling effect. The positive association may point to the presence of urban heat islands close to bodies of water as the reason for the higher temperatures in these places. **2022**: A weakly positive link is indicated

by the correlation, which shifts to 0.2142. This unpredictability may result from altered land use practices near bodies of water or from particular meteorological circumstances that existed throughout the research period.

LST and SAVI:

2002: There is a high negative association (R^2 = -0.7250) between LST and SAVI. This suggests that lower LST is correlated with greater SAVI values, which imply better plants with less impact from the soil. **2022:** An extremely weak positive link is indicated by the correlation, which dramatically weakens to 0.1354. This implies that, maybe as a result of growing urbanization and a decline in green space, the function of soil-adjusted plants in cooling the land surface has decreased.

LST and NDBI:

2002: There is a very significant positive association (R^2 = 0.8910) between LST and NDBI. Urban areas considerably raise land surface temperatures, as seen by the correlation between greater LST and higher NDBI values, which reflect built-up regions.

2022: An even greater association is indicated by the correlation, which increases to 0.9927. This indicates that built-up regions are contributing more to higher temperatures, suggesting an intensification of the urban heat island effect.

Table 5: LST with Normalized Indices soil may be a factor in rising temperatures.

Year	Indi	LST	NDVI	NDWI	SAVI	NDBI	BI
2002	LST	1.0000	-0.6530	0.4140	-0.7250	0.5931	0.7580
	NDV	-0.7320	1.0000	-0.7841	0.9085	-0.8671	-0.8282
	NDI	0.6321	-0.7746	1.0000	0.8510	-0.8157	-0.7819
	SAVI	-0.7203	0.9078	-0.8487	1.0000	-0.8813	-0.9265
	NDB	0.8871	-0.8656	0.6555	-0.9288	1.0000	0.9477
	BI	0.7510	-0.8281	0.5979	-0.9228	0.9918	1.0000
2022	LST	1.0000	−0.5453	0.2142	0.1354	0.6672	0.6564
	NDV	−0.5453	1.0000	−0.7087	1.0000	−0.7791	−0.8248
	NDI	−0.1609	−0.7087	1.0000	−0.7214	0.1481	0.8252
	SAVI	0.7354	1.0000	−0.7214	1.0000	−0.7698	0.4390
	NDB	0.9927	−0.7791	0.1481	−0.7798	1.0000	0.6073
	BI	0.7564	−0.8248	0.8252	0.3247	0.2633	1.0000

LST and BI:

2002: There is a high positive connection (R^2 = 0.7580) between LST and BI. Higher LST is correlated with areas with higher BI values, which indicate more bare soil, indicating that bare **2022**: There is a moderately favorable link, as seen by the correlation dropping to 0.6564. This implies that although bare soil still has an influence on LST, other factors like greater urbanization or altered land use patterns may have lessened that impact.

Calculation of LST from Urban Indices:

The linear regression model used to forecast Land Surface Temperature (LST) based on urban indices (UI) is shown in Figure 9. LST and UI showed a considerable connection in the model, with an R^2 value of 0.89 suggesting a meaningful relationship. This substantial connection implies that, in spite of possible saturation problems that often impact indices such as NDVI, the link between LST and UI remained strong. The UI was positively associated with rising temperatures as it kept rising.

Using Landsat data from 2022, the linear regression model was verified and found to be in good agreement with established temperature trends shown in Figure 8. The model made a comparison between model-derived temperatures (Tmod) and satellite-observed temperatures (Tsat). Based on observations from 300 locations within the research region, the

analysis incorporated data from Landsat 8 thermal data and UI temperature readings in Figure 9. The model's ability to accurately forecast fluctuations in temperature was validated by this comparison.

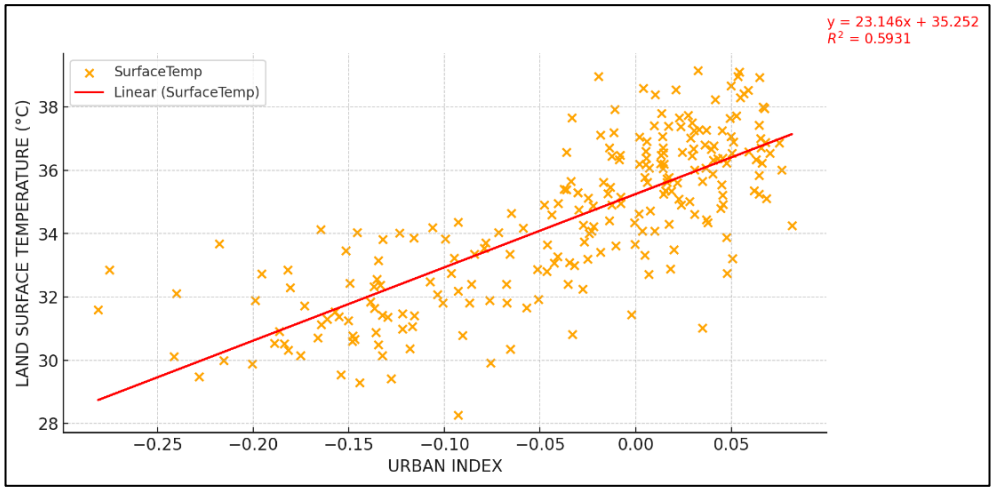

Figure 9: Linear Regression Model LST and UI

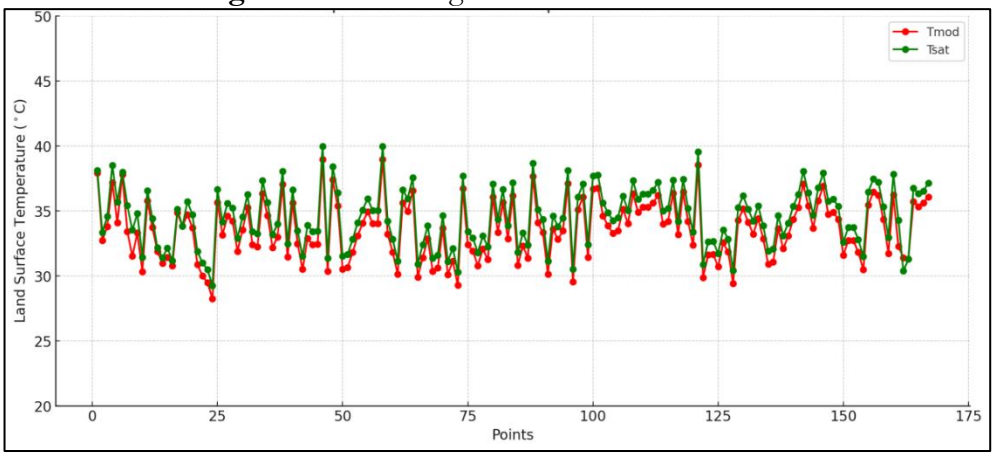

Figure 10: Comparisons between TMOD and TSAT

LST and LULC Prediction for 2042:

Prediction and Distribution of LULC and LST in Mardan 2042:

LULC 2042:

The projections of the CA-Markov chain model for changes in land use and land cover (LULC) between 2042 are shown in Figure 11. According to the model, there will be a rise in populated regions that will encroach on natural areas, vegetation, and water bodies. Green spaces may ultimately be replaced by buildings if present patterns continue, as has been noted in the past. Table 8 projects a large increase in the area covered by built-up areas by 2042. Between 2022 and 2042, the CA-Markov model projects that vegetation areas would shrink from 793.09 km² to 747.66 km², while built-up areas will increase from 266.70 km² to 299.99 km². The principal forces behind future growth include this increase in populated regions as well as reductions in water, vegetation, and bare land.

Table 6: Area Statistics of Predicted LULC for 2042

Classes Names	Area in Km²	Percentage %
Water Bodies	38.3228	2.34
Vegetation	747.6607	45.65
Built-up	299.9938	18.32
Barren Land	551.8851	33.70

Changes from 2022 to 2042 in Land Use Land cover:

Between 2022 and 2042, there will be noticeable changes in Mardan's land cover, according to the CA Markov model. A striking change from undeveloped to developed territory, or from barren to built-up, occurs in the northwest corner of the area, change expected is about 24.2 square kilometers, or 1.48% of the whole. Also, 12.28%, or 20.9 square kilometers, of formerly undeveloped area is expected to become vegetated. Bare land changing into water bodies (BA to WB) accounted for a mere 0.76 square kilometers, or 0.05%, of the total area affected.

The northern section, which accounts for 25.7 square kilometers, or 1.57% of the total area, is expected to experience a noteworthy transition from vegetation land to barren land (VG to BA). This change can occur over the whole region. Also, in the middle and eastern sections, there is an expectation of significant transition from vegetative to built-up regions, which accounts for 20.9 square kilometers, or 1.28%. With an impact of just half a square kilometer, or 0.03%, changes in bodies of water turning into barren land (WB to BA) were insignificant. Due to continuous urbanization and changes in land use patterns, this data-driven and spatially-oriented study emphasizes the ever-changing character of Mardan's land cover.

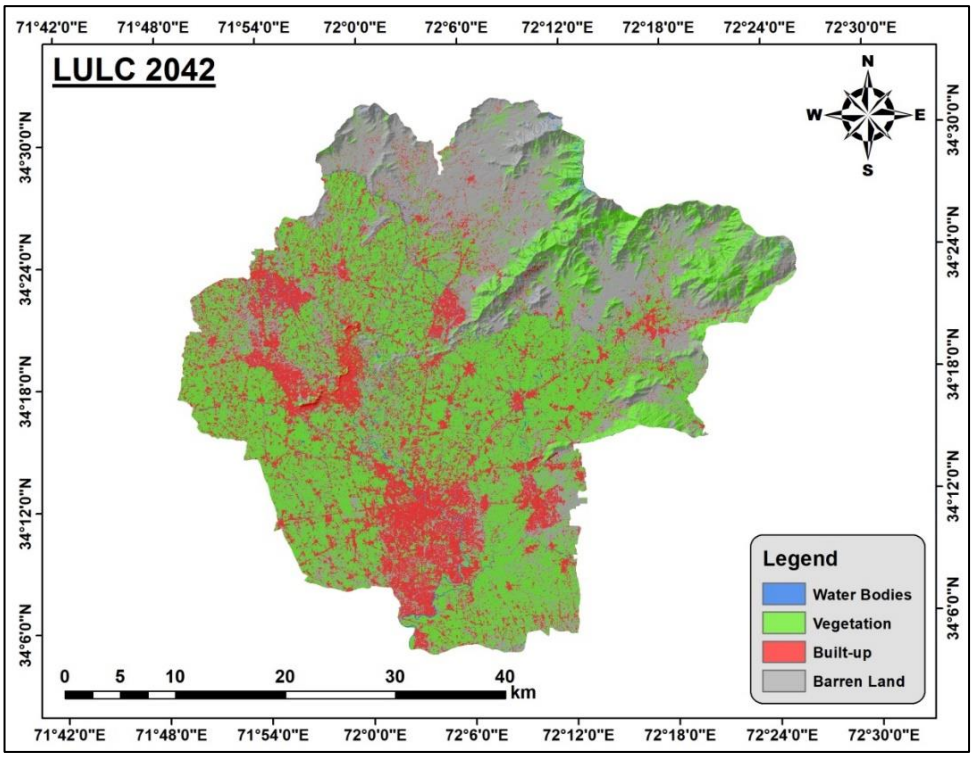

Figure 11: Predicted LULC from CA Markov Model for 2042

LST 2042:

The predicted trend in land surface temperature (LST) from 2022 to 2042 is also depicted in Figure 11. The growth in built-up areas is attributed by the model to fluctuations in LST throughout this era. It is anticipated that the lower LST classes would decrease as the extent of high LST locations (more than 35.581 °C) increases. In comparison to populated areas, it is anticipated that the vegetated western regions will continue to be colder. Higher LST classes (31.117 - 33.182 °C, 33.183 - 35.58 °C and 35.581 - 41 .531 °C) are predicted to replace the maximum region with low LST (20.454 - 28.719 °C and 28.72 - 31.116 °C). Table 4 indicates that major temperature rises are most likely to occur in the Southern, northern and north eastern regions, with most places perhaps moving into high-temperature categories (over 35.581 °C).

Table 7: Changes of different LULC classes which are predicted from CA Markov

Classes 2022	Classes 2042	Change Classes	Change Area SqKm	Change %
Barren Land	Barren Land	No Change	475.75	29.06
Barren Land	Built-up	BA To BU	24.20	1.48
Barren Land	Vegetation	BA To VG	20.88	1.28
Barren Land	Water Bodies	BA To WB	0.76	0.05
Built-up	Built-up	No Change	263.55	16.10
Vegetation	Barren Land	VG To BA	47.79	2.92
Vegetation	Built-up	VG To BU	47.97	2.93
Vegetation	Vegetation	No Change	711.23	43.45
Water Bodies	Barren Land	WB To BA	9.58	0.59
Water Bodies	Vegetation	WB To VG	4.57	0.28
Water Bodies	Water Bodies	No Change	30.57	1.87

The model predicts that between 2022 and 2042, the 20.454 - 28.719 °C temperature range would decrease from 100.05 km² to 84.8367 km², while the 35.581 - 41 .531 °C LST range will increase from 256.14 km² to 320.8833 km². Over time, it is predicted that temperatures in the upper group (over 23 °C) would rise at the cost of those in the lower category. This is especially clear from Figure 11, which depicts a notable increase in temperature in populated regions. Most low LST zones (20.454 - 28.719 °C and 28.72 - 31.116 °C) are predicted to move into high LST categories (33.183 - 35.58 °C and 35.581 - 41 .531 °C). As a result, even while the zone with lower LST may shrink, many places, particularly in the center, north, northwest and northeast, could go toward warmer temperatures—higher than 35.581°C as seen in Table 8.

Table 8: Area statistics of predicted LST for 2042

Classes Range	Area in Km²	Percentage %
20.454 - 28.719 (VL)	84.8367	5.18
28.72 - 31.116 (L)	327.3489	20.00
31.117 - 33.182 (M)	461.2779	28.18
33.183 - 35.58 (H)	442.5156	27.03
35.581 - 41 .531 (VH)	320.8833	19.60

Changes in LST from 2022 to 2042:

There are noticeable regional differences in the changes to Mardan's land surface temperature (LST) expected from 2022 to 2042. Initially classed as very low (VL) temperatures, 4.57 Km^2 would like to shift to moderate (VL to M) and 4.26 Km^2 to high temperatures (VL to H), making up 0.28% and 0.26% of the total area, respectively, after making this transformation. Also, very high temperatures (VL to VH) would shift into a smaller region of 0.03 Km^2, which is about 0.002% of the whole area. Also, low-temperature (L) areas is expected to change, going through noticeable shifts to high-temperature (L to H) and moderate-temperature (L to M) classes; these states account for 0.83% and 0.42% of the total area, and encompass 13.6 and 6.8 Km^2, respectively. Specifically, 13.3 Km^2 in central Mardan and 0.2 Km^2 in northern Mardan are expecting to see transitions from moderate to high and very high temperatures, respectively, from M to H and VH.

In addition, 2.4 Km^2, or 0.15 percent of the landmass, will be experiencing very high temperatures (VH), marking a substantial change from high temperatures (H). Over the past twenty years, land surface temperatures will be expected to rise in several parts of Mardan, and these geographical shifts are indicative of that tendency. It is clear from the statistics that urbanization and possible climate change variables are having an effect on local temperature variances, since there has been a move towards higher temperature classes.

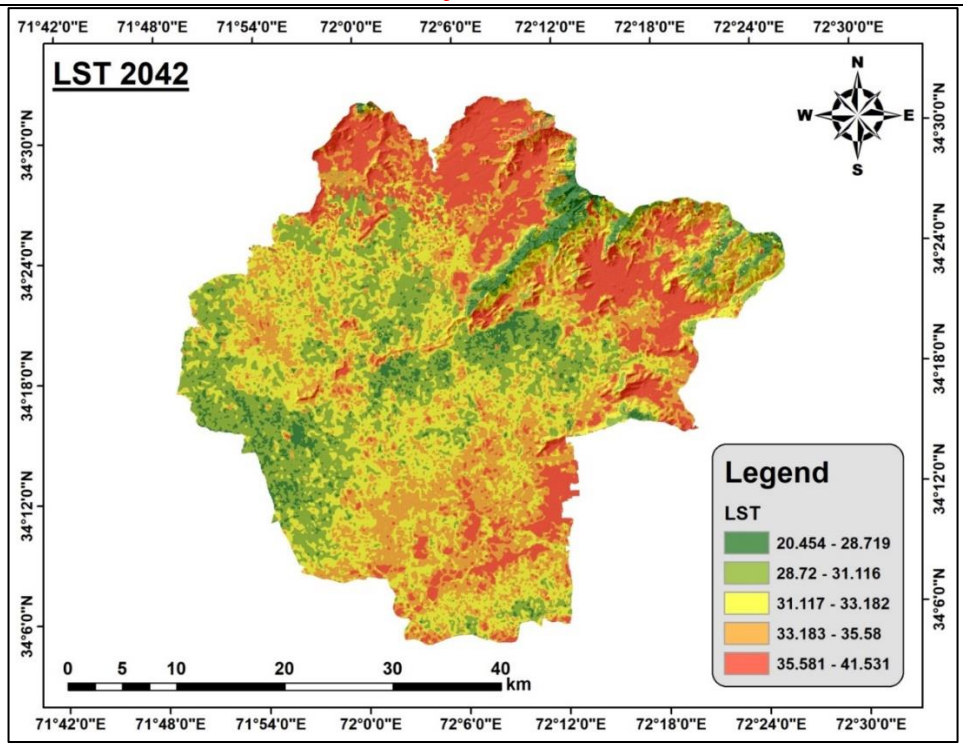

Figure 12: Predicted LST from CA Markov Model for 2042

Table 9: Changes of different LST classes which are predicted from CA Markov

Class 2022	Class 2042	Change Classes	Change Area (Sq.Km)	Change %
VL	VL	VL To VL	81.65	4.99
VL	L	VL To L	8.67	0.53
VL	M	VL To M	4.57	0.28
VL	H	VL To H	4.26	0.26
VL	VH	VL To VH	0.03	0.00
L	VL	L To VL	2.68	0.16
L	L	L To L	280.34	17.13
L	M	L To M	54.29	3.32
L	H	L To H	16.67	1.02
L	VH	L To VH	7.16	0.44
M	VL	M To VL	0.11	0.01
M	L	M To L	38.48	2.35
M	M	M To M	392.35	23.97
M	H	M To H	39.60	2.42
M	VH	M To VH	23.56	1.44
H	VL	H To VL	0.00	0.00
H	L	H To L	0.01	0.00
H	M	H To M	11.12	0.68
H	H	H To H	376.63	23.01
H	VH	H To VH	38.86	2.37
VH	H	VH To H	4.61	0.28
VH	VH	VH To VH	250.87	15.33

Discussions:

In order to anticipate land usage, land cover, and land surface temperature (LST) in Mardan, Khyber Pakhtunkhwa, Pakistan, this study used Markov chain models based on cellular automata. The ability of many land cover indexes to forecast variations in temperature

over time was evaluated. Following the Soil-Adjusted Vegetation Index (SAVI), the Normalized Difference Vegetation Index (NDVI), the Normalized Difference Built-up Index (NDBI), and the Built-up Index (BI), among others, the results showed that the Normalized Difference Water Index (NDWI) was the most accurate predictor of LST distribution.

The growth of city centers and the temperature of its environs were predicted using linear regression techniques. As long as there was no relationship between the predicted variables, multiple linear regressions were considered suitable. Considering the interdependence of the other factors, the Urban Index (UI) proved to be the most accurate temperature predictor. In order to calculate the possible environmental impact of LST, the UI model was used to predict the growth of urbanization and its future trajectory. The model projected temperatures with an average absolute error of 1.83 °C using LST data from the thermal band and a linear model adding UI. Recent research has demonstrated a strong correlation between the accuracy of UI's heat forecasts from urban growth and a number of other measures of urban expansion.

Although prior research had not confirmed the relationship between temperature and UI, the higher temperatures in locations with more built-up buildings and less greenery can be ascribed to the substantial predictive power demonstrated in this study. Water-intensive and residential regions in Colombo and Sri Lanka have comparable high urban indices. The high link between UI and LST can be explained by research showing that home water and energy use is strongly impacted by the intensity of urban climates. In 1990 and 2018, the Support Vector Machine (SVM) classifier was evaluated to achieve high-accuracy classification of urban land use and land cover (LULC) distribution. Additionally, a recent study showed that the SVM classifier was capable of producing extremely accurate maps. A map with more precision than the necessary 80% accuracy level was produced by using digitized areas rather than points as the ground data for categorization.

The LULC maps created in 2002 and 2022 showed that although residential areas grew, the amount of vegetation cover in the same area decreased. This result is consistent with earlier research. The great degree of agreement between the 2022 projected map and the map made with supervised classification techniques shows that the land cover and land use categories are accurately predicted by the CA-Markov chain model. The CA-Markov chain model projected that built-up areas will continue to grow until 2042 at the expense of land cover, unless policies such implementing green spaces, cropland, and water conservation are put in place. This prediction was based on changes in LULC between 1990 and 2018. This forecast is consistent with predictions from throughout the world that indicate the increase of the human population will keep uppacing the spread of natural areas. The research also forecasted an increase in the areas classified as having higher temperatures (31–35 °C and 35–41 °C), while the regions with the lowest temperature levels are likely to fall. As more people live in cities, there will be less green space and water available, which is in line with patterns found in earlier research.

The results of this study are essential for changing Khyber Pakhtunkhwa's urban planning and management. These changes will improve the district's reputation by addressing issues like land record management, solid waste management infrastructure, capacity building, landfill construction and development, pond removal, and assistance for union councils or local government in rehabilitating dangerous buildings.

Conclusion:

Significant changes brought about by urbanization are revealed by the spatiotemporal analysis of Land Use and Land Cover (LULC) in the Mardan area from 2002 to 2022. The study's conclusions show that there has been a significant rise in built-up areas from 165.47 km² to 266.70 km² at the expense of vegetative and agricultural grounds. Vegetation dropped from 928.76 km² to 793.09 km² during the same time. The constant trade-off between urban

growth and the natural land cover is highlighted by these modifications. Overall accuracy (OA) increased from 81% in 2002 to 87% in 2022, indicating that the accuracy evaluation validates the validity of these results. This illustrates how reliable the study's Maximum Likelihood Classification (MLC) algorithm is. The effects of increasing urbanization on the environment are highlighted by the decrease in vegetative cover and the rise in arid and built-up areas.

Furthermore, a discernible trend of rising temperatures over the previous 20 years is shown by the Land Surface Temperature (LST) data. From 25–36°C in 2002 to 20–41°C in 2022, the average LST range changed, with the highest temperatures becoming more often. The positive association between LST and urban indices (UI) suggests a direct relationship between the rise in built-up areas and the decrease in vegetative cover caused by this temperature increase. The CA-Markov model projections for 2042 indicate that built-up areas will continue to rise, reaching 299.99 km², while vegetative cover will continue to drop, reaching 747.66 km². Additionally, a surge in high LST zones is predicted by the model, with notable spots perhaps seeing temperatures above 35.58°C. With regard to reducing the negative impacts of urbanization on the climate and land use, these projections highlight the urgent need for sustainable urban design and environmental conservation measures. In order to balance growth and environmental sustainability, this study highlights the significance of incorporating green spaces and water bodies into urban development plans. Overall, it offers important insights into the dynamic changes in land use and temperature in the Mardan neighborhood. The results can help policymakers make well-informed choices that will improve urban sustainability and resilience in the face of ongoing development and climate problems.

References

[1] S. Liu et al., "Understanding Land use/Land cover dynamics and impacts of human activities in the Mekong Delta over the last 40 years," Glob. Ecol. Conserv., vol. 22, p. e00991, Jun. 2020, doi: 10.1016/J.GECCO.2020.E00991.

[2] M. M. H. Seyam, M. R. Haque, and M. M. Rahman, "Identifying the land use land cover (LULC) changes using remote sensing and GIS approach: A case study at Bhaluka in Mymensingh, Bangladesh," Case Stud. Chem. Environ. Eng., vol. 7, p. 100293, Jun. 2023, doi: 10.1016/J.CSCEE.2022.100293.

[3] E. F. Lambin and H. Geist, Eds., "Land-Use and Land-Cover Change," 2006, doi: 10.1007/3-540-32202-7.

[4] "(PDF) Land use/land cover change detection and prediction using the CA-Markov model: A case study of Quetta city, Pakistan." Accessed: Jun. 22, 2024. [Online]. Available: https://www.researchgate.net/publication/355209516_Land_useland_cover_change_detection_and_prediction_using_the_CA-Markov_model_A_case_study_of_Quetta_city_Pakistan

[5] "Urban Climate | Journal | ScienceDirect.com by Elsevier." Accessed: Jun. 22, 2024. [Online]. Available: https://www.sciencedirect.com/journal/urban-climate

[6] "Temporal March of the Chicago Heat Island in: Journal of Applied Meteorology and Climatology Volume 24 Issue 6 (1985)." Accessed: Jun. 22, 2024. [Online]. Available: https://journals.ametsoc.org/view/journals/apme/24/6/1520-0450_1985_024_0547_tmotch_2_0_co_2.xml

[7] X. L. Chen, H. M. Zhao, P. X. Li, and Z. Y. Yin, "Remote sensing image-based analysis of the relationship between urban heat island and land use/cover changes," Remote Sens. Environ., vol. 104, no. 2, pp. 133–146, Sep. 2006, doi: 10.1016/J.RSE.2005.11.016.

[8] R. Wang, H. Hou, Y. Murayama, and A. Derdouri, "Spatiotemporal Analysis of Land Use/Cover Patterns and Their Relationship with Land Surface Temperature in

Nanjing, China," Remote Sens. 2020, Vol. 12, Page 440, vol. 12, no. 3, p. 440, Jan. 2020, doi: 10.3390/RS12030440.

[9] P. Ghosh et al., "Application of Cellular automata and Markov-chain model in geospatial environmental modeling- A review," Remote Sens. Appl. Soc. Environ., vol. 5, pp. 64–77, 2017, doi: 10.1016/j.rsase.2017.01.005.

[10] B. Nath, Z. Wang, Y. Ge, K. Islam, R. P. Singh, and Z. Niu, "Land Use and Land Cover Change Modeling and Future Potential Landscape Risk Assessment Using Markov-CA Model and Analytical Hierarchy Process," ISPRS Int. J. Geo-Information 2020, Vol. 9, Page 134, vol. 9, no. 2, p. 134, Feb. 2020, doi: 10.3390/IJGI9020134.

[11] D. J. Guan, H. F. Li, T. Inohae, W. Su, T. Nagaie, and K. Hokao, "Modeling urban land use change by the integration of cellular automaton and Markov model," Ecol. Modell., vol. 222, no. 20–22, pp. 3761–3772, Oct. 2011, doi: 10.1016/J.ECOLMODEL.2011.09.009.

[12] X. Yang, X. Q. Zheng, and L. N. Lv, "A spatiotemporal model of land use change based on ant colony optimization, Markov chain and cellular automata," Ecol. Modell., vol. 233, pp. 11–19, May 2012, doi: 10.1016/J.ECOLMODEL.2012.03.011.

[13] J. Huang, Y. Wu, T. Gao, Y. Zhan, and W. Cui, "An Integrated Approach based on Markov Chain and Cellular Automata to Simulation of Urban Land Use Changes," Appl. Math. Inf. Sci, vol. 9, no. 2, pp. 769–775, 2015, doi: 10.12785/amis/090225.

[14] F. Fan, Y. Wang, and Z. Wang, "Temporal and spatial change detecting (1998-2003) and predicting of land use and land cover in Core corridor of Pearl River Delta (China) by using TM and ETM+ images," Environ. Monit. Assess., vol. 137, no. 1–3, pp. 127–147, Jun. 2008, doi: 10.1007/S10661-007-9734-Y/METRICS.